ELSEVIER

Polymer 42 (2001) 9679–9686

polymer

www.elsevier.com/locate/polymer

Properties of highly syndiotactic poly(vinyl alcohol)

Yoshitaka Nagara[a,1], Tamaki Nakano[b], Yoshio Okamoto[c,*], Yasuo Gotoh[d], Masanobu Nagura[d]

[a]*Joint Research Center for Precision Polymerization (JRCPP), Japan Chemical Innovation Institute (JCII), Graduate School of Engineering, Nagoya University, Furo-cho, Chikusa-ku, Nagoya 464-8603, Japan*

[b]*Graduate School of Materials Science, Nara Institute of Science and Technology (NAIST), Takayama-cho 8916-5, Ikoma, Nara 630-0101, Japan*

[c]*Department of Applied Chemistry, Graduate School of Engineering, Nagoya University, Furo-cho, Chikusa-ku, Nagoya 464-8603, Japan*

[d]*Faculty of Textile Science and Technology, Shinshu University, 3-15-1, Tokida, Ueda 386-8567, Japan*

Received 13 April 2001; received in revised form 8 June 2001; accepted 2 July 2001

Abstract

The physical properties of a highly syndiotactic poly(vinyl alcohol) (PVA, diad syndiotacticity (r) = 69%) and a commercial, atactic PVA (r = 54%) were examined. The highly syndiotactic PVA was derived from poly (vinyl acetate) prepared through the radical polymerization of vinyl acetate in $(CF_3)_2CHOH$. The solubility, gelation behavior, melting point, and crystallization rate were drastically affected by the tacticity of the main chain. Some of the properties were measured using fiber samples prepared by the gel spinning technique. The fiber obtained from the syndiotactic PVA had a melting point of 274°C. This is the highest melting point reported for PVA. These effects of tacticity on the polymer properties are ascribed to the difference in intermolecular and/or intramolecular hydrogen bonding. A polymer chain with higher r content may form more regular and therefore more rigid hydrogen bonding between the polymer chains in the bulk sample. Such a detailed study on the effects of tacticity on the properties of PVA has not been reported so far.

Keywords: Poly(vinyl alcohol); Syndiotacticity; Physical property

1. Introduction

The stereostructure of a polymer chain often significantly affects the physical properties of the polymer. Therefore, when one designs a macromolecular material, it is important to consider the tacticity of the source polymer as well as its molecular weight and chemical composition. Poly(vinyl alcohol) (PVA) is widely used as fibers, films, adhesives, and substitutes for asbestos, and the effect of tacticity on the physical properties is known to be especially significant. An increase in the syndiotacticity of PVA has been reported to improve the physical properties such as heat resistance, tensile strength, and the modulus [1–10]. In particular, the solubility in solvents and the melting temperature of PVA are significantly influenced by the tacticity. For example, syndiotacticity-rich PVA is insoluble in boiling water [11], which is well known to be a good solvent for atactic PVA. Furthermore, the melting temperature of PVA is increased with increase in both the syndio- and isotacticities [1–5,12–16]. As for syndiotacticity- rich PVAs, Fukae et al. reported the relationship between melting point and syndiotacticity using the polymer derived from poly(vinyl pivalate) [7,8]. Murahashi et al. reported the highest melting temperature of 286°C for PVA having a diad syndiotacticity (r) of 74% [13–16]. The PVA with r = 74% has been obtained by saponification of poly(vinyl trimethylsilyl ether) synthesized by cationic polymerization. However, the monomer is not readily available and difficult to handle because it is easily hydrolyzed even by the moisture in the air, and the PVA had a lower degree of polymerization of 300. Thus, it is difficult to use the PVA for practical use. On the other hand, we reported that PVA with r = 72% can be prepared by saponification of poly(vinyl acetate) which is produced by the radical polymerization of vinyl acetate (VAc) in $(CF_3)_3COH$ [17,18]. The PVA of r = 72% exhibited a melting temperature of 269°C, which is higher than that of commercially available atactic PVAs having r = 52–54% (220–235°C). We also prepared PVA with r = 69% by using $(CF_3)_2CHOH$ instead of $(CF_3)_3COH$ as a solvent for the radical polymerization of VAc. $(CF_3)_2CHOH$ is much cheaper than $(CF_3)_3COH$, and therefore, it is advantageous for producing a syndiotacticity-rich PVA in a large quantity. In fact, several hundred grams of PVA with r = 69% has been obtained using $(CF_3)_2CHOH$ as we have

* Corresponding author. Tel.: +81-52-7894600; fax: +81-52-7893188.
E-mail address: okamoto@apchem.nagoya-u.ac.jp (Y. Okamoto).
[1] R & D Center, Unitika Ltd., 23 Kozakura, Uji, Kyoto 611-0021, Japan.

0032-3861/01/$ - see front matter
PII: S0032-3861(01)00493-1

recently reported [19]. The physical properties of the PVA having such a high *r* content have not yet been investigated in detail.

In this study, some physical properties of PVA with $r = 69\%$ were studied in comparison with a commercially available atactic PVA with $r = 54\%$. The properties examined in this study include solubility, viscosity, gelation behavior, thermal properties, and mechanical properties.

2. Experimental

2.1. PVA samples

The highly syndiotactic PVA with $r = 69\%$ and the atactic PVA with $r = 54\%$ used in this study are denoted as sPVA and aPVA, respectively. The synthesis of sPVA was described in detail in our recent publication [19]. aPVA was supplied from Unitika Ltd. and used after resaponification. The hydrolysis yields of the both polymers were quantitatively as determined by ^{1}H NMR analysis.

2.2. Spinning of PVA fibers

PVA fibers were produced from dimethyl sulfoxide (DMSO) solutions of PVAs by the gel spinning technique. Spinning solutions were prepared by dissolving sPVA and aPVA in DMSO at 150°C. The concentrations of sPVA and aPVA solutions were 5 and 15 wt%, respectively. The spinning solution kept at 120°C was extruded from the nozzle with a diameter of 0.5 mm and an *L/D* ratio of 5 into the coagulation bath filled with methanol by applying a nitrogen gas pressure. The temperature of methanol as coagulating agent was −40°C. The obtained fiber was wound up using a roller and stored in methanol for several days to remove residual DMSO. After removal of DMSO, the fiber was cut into pieces and dried at room temperature to remove methanol. Drawing of the fibers was performed in a hot oven using a hand-operated drawing device. The sPVA and aPVA fibers were drawn out to 20 times the original length at 240°C and to 15 times the original length at 215°C, respectively. Some of the sPVA fibers drawn 20 times the original length were further drawn up to 1.5 times at 260°C, that is, the sPVA fibers with a total draw ratio of 30 were produced. It was necessary to draw the sPVA fibers as fast as possible because sPVA became brittle by heating due to fast crystallization (see Section 3). After the drawing is completed, the fibers were kept at the drawing temperature for 3 min in the oven.

2.3. Measurements

The tacticity of the PVAs was determined by ^{13}C NMR spectra recorded on a Varian UNITY-INOVA spectrometer (125 MHz) in DMSO-d_6 at 80°C. Fig. 1(a) and (b) shows the ^{13}C NMR spectra of sPVA and aPVA, respectively. Triad tacticity was estimated on the basis of the intensity ratio of

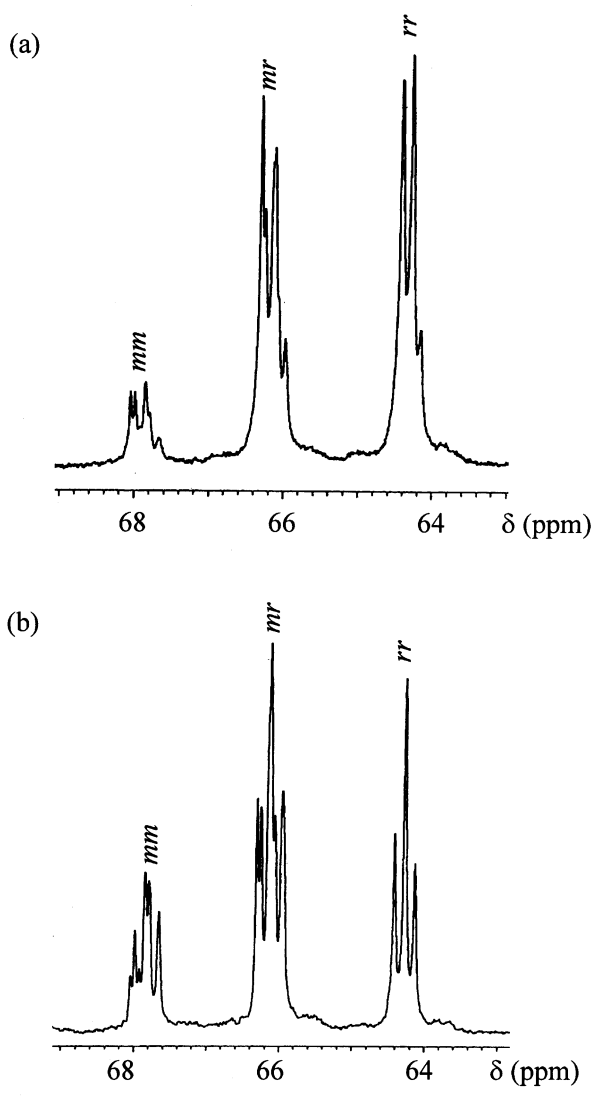

Fig. 1. 125 MHz ^{13}C NMR spectra (methine region) of: (a) sPVA ($r = 69\%$), (b) aPVA ($r = 54\%$) in DMSO-d_6.

three groups of peaks due to the methine carbon in the main chain.

The number average molecular weight (M_n) and polydispersity (M_w/M_n) of the starting poly(VAc)s were determined by size-exclusion chromatography (SEC) calibrated with standard polystyrenes using a chromatograph equipped with a Jasco PU-980 pump, a Jasco RI-930 detector, and TSKgel GMH_{HR}-H and $G3000H_{HR}$ columns connected in series (eluent; THF, temperature; 40°C). DP of the PVAs was calculated using the M_n values determined for the poly(VAc)s. The structural characteristics of the two PVAs are summarized in Table 1.

The viscosity of DMSO solutions of PVA was measured by a TOKIMECVISCOMETER TV-20 from 120°C to room temperature. The measurement temperature was controlled stepwise, and the viscosity was read off 10 min after the desired temperature reached. The spindle of the viscometer was rotated at 10 rpm.

Table 1
Structural characteristics of sPVA and aPVA

	M_n[a] $\times 10^{-3}$	M_w/M_n[a]	DP[b]	Tacticity[c]			
				mm	*mr*	*rr*	*r*
sPVA	114	2.7	1300	8.5	44.6	46.9	69.2
aPVA	110	2.2	1250	21.0	50.3	28.7	53.8

[a] Determined by SEC of poly(VAc) (PSt standard, THF).
[b] Calculated based on M_n (DP = $M_n/(M_n$ of VAc monomer)).
[c] Determined by 125 MHz ^{13}C NMR of PVA in DMSO-d_6.

The melting point and the crystallization point of polymers were determined using a SEIKO SSC5200 differential scanning calorimeter at a cooling and heating rate of 10°C/min in a nitrogen flow. The isothermal crystallization experiment was performed using a Perkin Elmer DSC-7 differential scanning calorimeter in a nitrogen flow. The Avrami constant (n), which depended on the mechanism of nucleation and growth of crystals, was determined according to the following equation [20–23]:

$$1 - \theta = \exp(-Zt^n) \quad (1)$$

where θ is (crystallinity at time t)/(crystallinity at infinity of time), and Z is a rate constant. Eq. (1) was rewritten as follows:

$$\log(-(1 - \theta)) = n \log t + A \quad (2)$$

Thermal mechanical analysis (TMA) of as-spun PVA fibers was measured using a SEIKO SS-10 at a heating of 5°C/min under a tension of 1 MPa in a nitrogen flow.

The wide-angle X-ray diffraction (WAXD) patterns of sPVA and aPVA were recorded on a Rigaku RU-300. The monochromatic CuKα radiation was used with the X-ray generator power of 50 kV at 300 mA.

Tensile properties of the fiber were measured using an Orientic Tensilon UTM-II-20. Fiber samples of 10 mm length prepared at a drawing rate of 10 mm/min were used.

Optical birefringence was measured using a NIKON polarizing microscope with a Wetzer compensator. Birefringence was determined according to the following equations:

$$\Delta n = \Gamma/d_0 \quad (3)$$

$$\Gamma = \frac{c}{10^4} \times 10^4 f(i) \quad (4)$$

$$i = \frac{a - b}{2} \quad (5)$$

where d_0 is the diameter of the fibers, $c/10^4$ (0.764) the constant for the compensator, and a and b are the measured values by polarizing microscope.

3. Results and discussion

3.1. Solubility of sPVA

Since PVA is often used in solution as crude material for fibers and films, its solubility in solvents is a most important property. Solvents such as water, DMSO, ethylene glycol, and glycerol have generally been utilized to dissolve PVA [1–5,12,24]. The solubility of PVA in solvents decreases with an increase in the syndiotacticity of the PVA molecules [1–5], because a syndiotactic sequence leads to the strong intermolecular hydrogen bond of PVA. Atactic PVA (r = 53%) is generally dissolved in hot water below 100°C, while PVA with a higher r value is insoluble in hot water at 100°C [25]. For example, PVA with r = 57.4% was dissolved in water at 127°C [12] and those with r = 65–70% at 150–160°C [25]. The solubility in four solvents of the as-obtained sPVA and aPVA is summarized in Table 2. The dissolution temperatures of PVA with a lower syndiotacticity (r = 57.4%) are shown in the table for comparison [12]. At a concentration of less than 1 wt%, sPVA was soluble in water at 200°C, which is considerably higher than the dissolution temperatures of the syndiotacticity-rich sPVAs ever reported. sPVA was also soluble in DMSO, ethylene glycol, and glycerol. The dissolution temperatures in these solvents were higher than those of aPVA and the PVA of r = 57.4%. The syndiotacticity-rich PVA with r = 64% has been reported to dissolve in *N*-methylmorpholine N-oxide/water = 70/30 (w/w) at 100°C [26], which is known to be a good solvent system for polymers having strong hydrogen bonds such as cellulose [27] and silk fibroin [28]. However, sPVA was not soluble in this solvent mixture at 100°C. Thus, the solubility of sPVA was lower than those of PVA with a lower syndiotacticity, suggesting that the intermolecular hydrogen bonding of sPVA tightly binds the polymer chains.

3.2. Viscosity of sPVA solution

Fig. 2(a) and (b) show the temperature dependences of viscosity for DMSO solutions of sPVA and aPVA, respectively. From Fig. 2(a), the viscosity of the sPVA solutions above 60°C slightly increased with a decrease of temperature. When the viscosity of sPVA solutions drastically

Table 2
Dissolution temperature for syndiotactic PVA (polymer concentration: 0.1 g dl^{-1})

	sPVA	Reference[a]
Diad syndiotacticity (r)	69.2	57.4
Degree of polymerization (DP)	1300	15 300
Water	200	127
DMSO	115	86
Ethylene glycol	> 200	153
Glycerol	> 200	164

[a] Data was cited from Ref. [12].

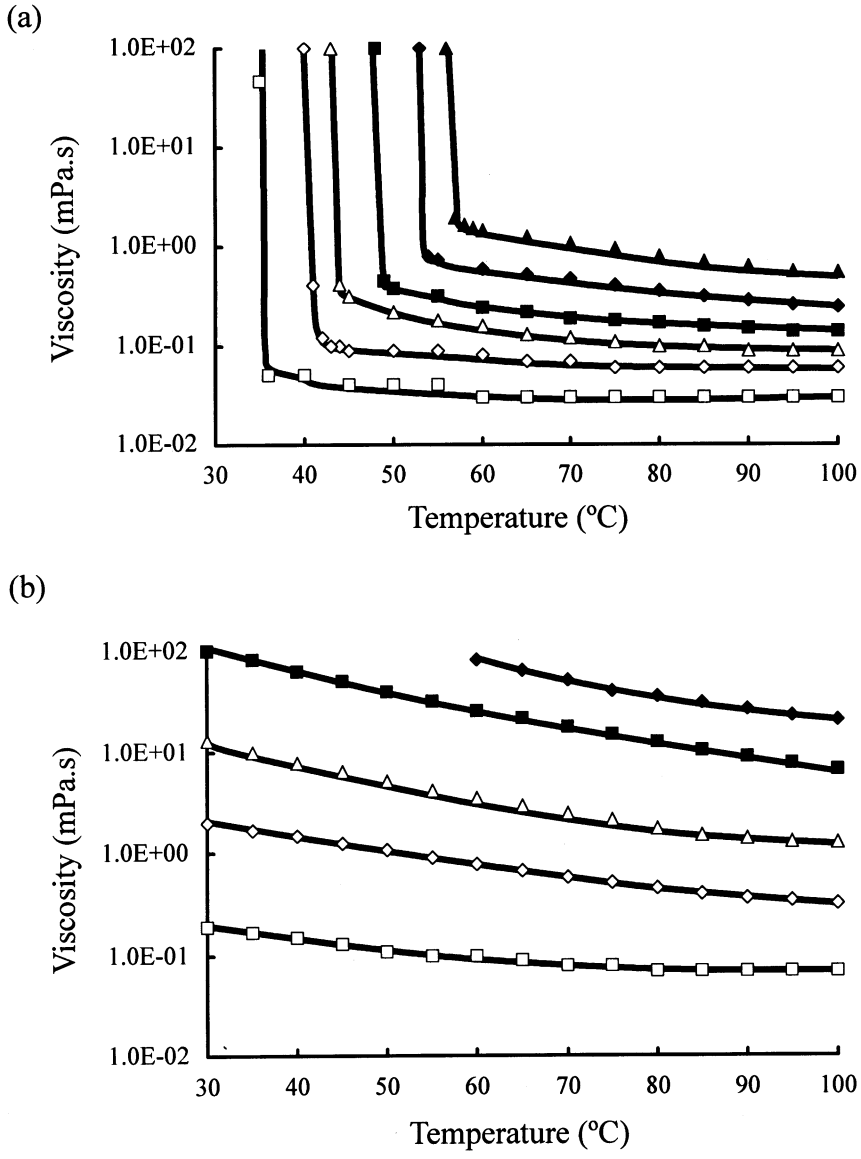

Fig. 2. Viscosity changes of: (a) sPVA DMSO solution at 6 wt% (▲), 5 wt% (◆), 4 wt% (■), 3 wt% (△), 2 wt%(◇), and 1 wt% (□). (b) aPVA DMSO solution at 25 wt% (◆), 20 wt% (■), 15 wt% (△), 10 wt% (◇), and 5 wt% (□).

increased with decrease of temperature, the gelation of the solutions took place. Gelation temperature in this study was determined as a temperature at which the viscosity drastically increased and went beyond the upper limitation of the viscometer. The gelation temperature was dependent on the sPVA concentration of the solutions. Fig. 3 shows the relationship between gelation temperature and concentration of the sPVA solutions.

With respect to the gelation of sPVA solution, a relatively stiff gel was formed even from a 1 wt% solution. In contrast, the behavior of the aPVA solutions ranging in concentration from 5 to 25 wt% was quite different from those of sPVA. As shown in Fig. 2(b), the viscosity of the aPVA solutions increased with a decrease in temperature. However, the

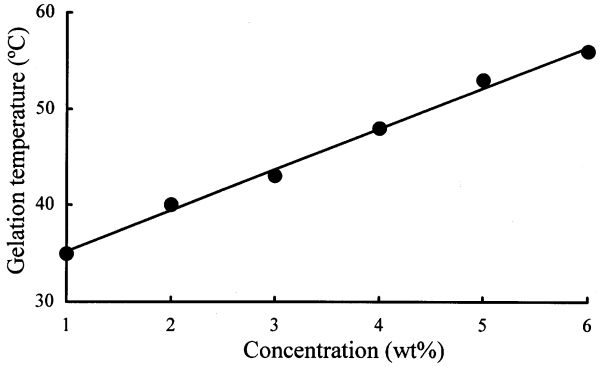

Fig. 3. Gelation temperatures of sPVA DMSO solution.

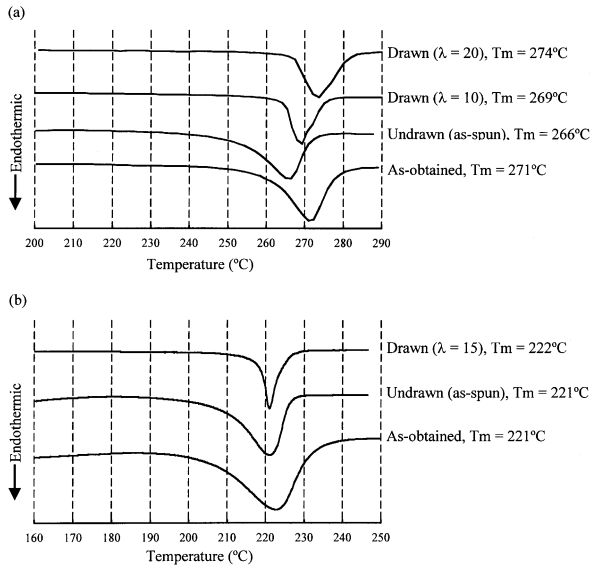

Fig. 4. DSC thermograms of: (a) sPVA and (b) aPVA fiber.

aPVA solutions, whose concentrations were much higher than those of the sPVA solution, did not gel in the temperature range measured in this study. In addition, it was noteworthy that the viscosity of the 5 wt% sPVA solution was higher by about one order than that of the 5 wt% aPVA solution although the PVAs have approximately the same degree of polymerization. These results strongly suggest that the hydrogen bonding of sPVA in the solution is stronger than that of aPVA, and this brought about the cohesive force of the sPVA molecules and the formation of insoluble crystallites in solution at a relatively high temperature. Thus, the crystallites formed in the sPVA solutions acted as physical crosslinking points and led to the gelation of the sPVA solutions.

3.3. Thermal properties of solid sPVA

The increase in the stereoregularity in PVA generally enhances the melting temperature, leading to a high heat resistance. Fig. 4(a) and (b) shows the DSC thermograms of the as-obtained samples and the as-spun or drawn fibers of sPVA and aPVA, respectively. The draw ratio (λ) of the drawn fibers is shown in the figures. The T_m of the as-obtained sPVA was about 50°C higher than that of the as-obtained aPVA. The T_m of the as-spun sPVA fiber was lower than those of the other sPVAs. The T_m of the sPVA fiber increased with an increase in the draw ratio and this is the same tendency as noted for the results of the highly syndiotactic PVA ($r = 64\%$) reported by Matsuzawa et al. [26]. The crystallization temperature (T_c) and heat of fusion were 239°C and 4.62 kJ mol^{-1} for the as-obtained sPVA, and 196°C and 3.74 kJ mol^{-1} for the as-obtained aPVA, respectively. For both the as-obtained and fiber samples, sPVA had a higher T_m, T_c, and ΔH when compared to the aPVA. This suggests that the intermolecular hydrogen bonding is stronger in sPVA based on the main-chain structure with a higher stereoregularity. The T_ms of the aPVA samples were almost constant, and the aPVA fiber drawn 15 times the original length exhibited a narrower transition peak than the other samples, which implies that the structure of the crystallites with a relatively uniform size distribution may form during the drawing process.

Fig. 5 shows the relationship between the diad syndiotacticity and T_m of PVAs with different tacticities that were synthesized in our laboratory including sPVA and aPVA. The monomers as starting materials and the polymerization solvents are indicated in the figure caption. In the range $r =$ 48–72%, T_m increased almost linearly from 220 to 271°C with an increase in the syndiotacticity. This implies that a

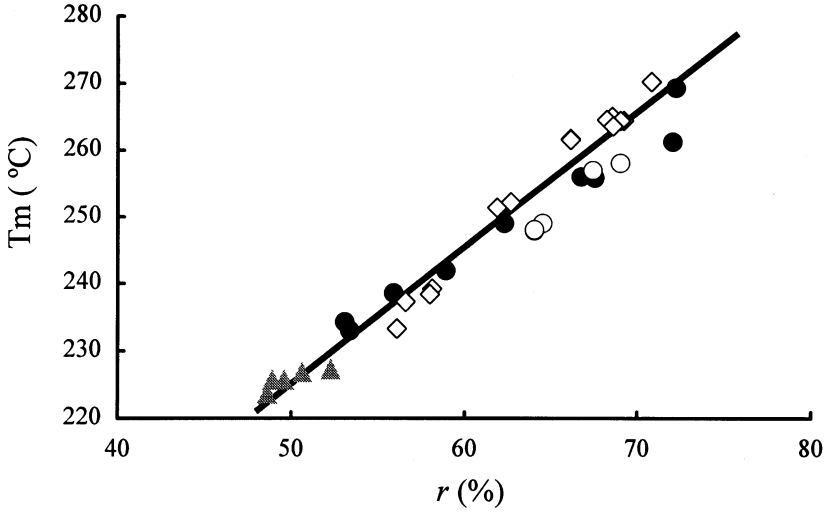

Fig. 5. Relationship between diad syndiotacticity (r) and melting point of PVA obtained through the polymerization of VAc in $(CF_3)_2CHOH$ (◇), VAc in $(CF_3)_3COH$ (●), VPi in $(CF_3)_3COH$ (▲), and VPi in *n*-hexane (○). The data for the polymers obtained using $(CF_3)_3COH$ and *n*-hexane as solvents were cited from Ref. [18].

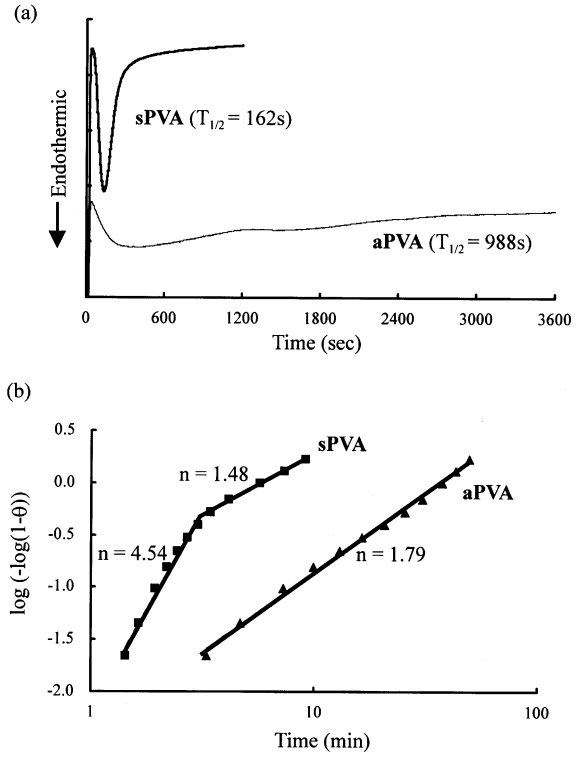

Fig. 6. (a) Isothermal crystallization thermograms of sPVA (bold line) and aPVA (faint line). (b) Avrami plots of: (a) sPVA (■) and (b) aPVA (▲).

further increase in the melting temperature may be expected when a higher syndiotacticity is realized.

Fig. 6(a) shows the isothermal crystallization thermograms for the as-obtained PVAs. Isothermal crystallization was performed at 250°C for sPVA and at 215°C for aPVA after melting at 280°C for 1 min and at 245°C for 2 min was conducted for sPVA and aPVA, respectively. For sPVA, the maximum for the endothermic peak appeared at 2 min and the crystallization was completed in 10 min. On the other hand, the endothermic peak of aPVA was much broader than that of sPVA and the crystallization process continued over the time range of 60 min. The half-value periods ($t_{1/2}$) of the crystallization were 162 s for sPVA and 988 s for aPVA. Thus, the crystallization of sPVA was found to be much faster than that of aPVA. This is consistent with the fact that during the drawing process of the sPVA fiber, the fiber became too brittle to be drawn when the fiber remained in a hot oven above 200°C for several minutes. The brittleness may be attributed to the formation of spherulites in the fiber due to the rapid procedure of crystallization of the sPVA. These results mean that the strong hydrogen bond of sPVA induces a high crystallization rate, and the period of drawing of highly syndiotactic PVA at high temperature should be as short as possible. This fact is considered very important in producing a high modulus and high strength fiber from sPVA.

Fig. 6(b) shows the Avrami plots for the as-obtained PVA samples, which are derived from the results in Fig. 6(a). From the plots, the crystallization of sPVA seems to proceed through two stages, whereas that of aPVA through a single stage. According to Eq. (2), the Avrami constants (n) were determined to be 4.54 and 1.48 at the first and the second stages, respectively, for sPVA, and 1.79 for aPVA. For sPVA, the crystal growth may be divided into the primary and secondary crystallizations. The larger n value of 4.54 at the first stage suggests a three-dimensional growth of the crystallite, that is, the formation of spherullites [20–23]. The n value at the second stage was 1.48, indicating that the crystal growth proceeds with a one- or two-dimensional crystallization. Since the n value of the second stage is smaller than 2, the crystallization rate is much smaller, and the lower dimensional crystal growth may proceed with heterogeneous nucleation. In this case, the crystallites formed during the first stage may act as a seed for crystal growth of the second stage. The crystallization of aPVA may proceed in the one-dimentsional growth manner with homogeneous nucleation, because the n value was close to 2. A similar assumption has been presented for the crystallization kinetics of an aqueous solution of syndiotacticity-rich PVA [29].

Fig. 7 shows the TMA thermograms for the undrawn PVA fibers. On the basis of the results, the inflecting points for the sPVA and aPVA fibers were found at 63 and 48°C, respectively. These temperatures are considered to correspond to the glass transition temperatures (T_g) [1–5]. The T_g of sPVA was higher than that of aPVA, indicating that the intermolecular hydrogen bond of sPVA is stronger not only in the crystalline regions but also in the amorphous regions than that of aPVA. The T_g of PVA has been reported to be classified into two temperature groups: about 75 and 85°C [4]. The thermal history of the samples may be the cause of the scattering of T_g. In addition, the water adsorption changes T_g, that is, T_g decreases with increase of water content in the sample. The T_gs in the present study are somewhat lower than those in the literature. For our PVAs, any heat treatment not conducted, thus the discrepancy of T_gs in this study from those ever reported may relate to thermal history and/or water adsorption.

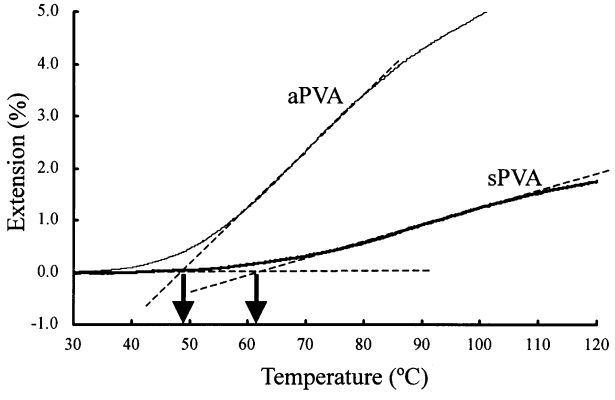

Fig. 7. TMA thermograms of sPVA (bold line) and aPVA (faint line).

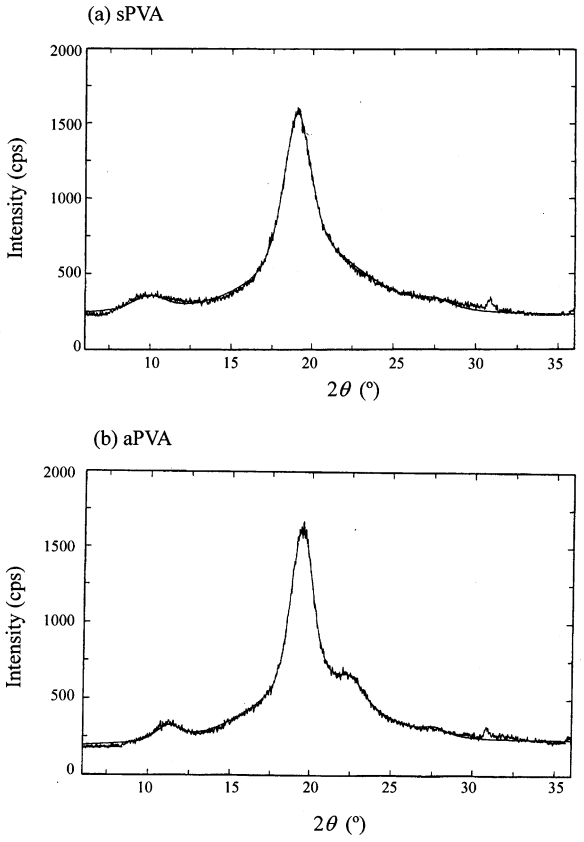

Fig. 8. Radial scatterings from: (a) sPVA and (b) aPVA powder.

3.4. WAXD pattern of sPVA

Fig. 8(a) and (b) shows the WAXD patterns of the as-prepared sPVA and aPVA, respectively. The pattern of sPVA is somewhat different from that of aPVA, that is, the positions of the peak maxima at $2\theta =$ ca. 10–11; and ca. 18–19° are not in agreement with each other. In addition, aPVA has a definite shoulder peak at about 22.5°, while sPVA does vaguely. The dependence of WAXD patterns of PVAs on the stereoregularity has been reported [30]. The origin of the difference in the WAXD patterns in this study is not immediately known. The crystal structure of a syndiotacticity-rich PVA with $r = 65\%$ has been reported to basically agree with Bunn's model for atactic PVA [31,32]. Furthermore, in our study, the pattern of sPVA after annealing at 200°C for 30 min was almost coincident with that of aPVA shown in Fig. 8(b). Thus, the crystal structure of sPVA seems to be the same as that of aPVA.

The crystallinities of the as-obtained sPVA and aPVA determined from the WAXD patterns were 38 and 34%, respectively. Crystallinity can also be estimated from the heat of fusion in the DSC curves. The crystallinity was calculated from ΔH obtained by DSC, assuming that the heat of fusion of the fully crystalline PVA is 6.87 kJ mol^{-1} regardless of the degree of syndiotacticity [33]. As a result, the crystallinites were 67% for sPVA and 55% for aPVA, respectively. The larger crystallinity by DSC than that by WAXD implies that the crystallization proceeded during the DSC measurements. In addition, the larger difference in the crystallinity from the DSC data suggests that sPVA crystallized more rapidly than aPVA during the heating process of the DSC measurements because of the stronger hydrogen bonding.

Table 3
Mechanical properties of sPVA and aPVA drawn fiber

	sPVA	aPVA
Draw ratio	30	15
Strength (GPa)[a]	1.43	1.49
Young modulus (GPa)[a]	38.1	25.2
Optical birefringence (10^{-3})[b]	35.5	35.3

[a] Determined by tensilon.
[b] Determined by polarizing microscope.

3.5. Mechanical properties of PVA fibers

The mechanical properties of PVA have been investigated by many researchers because the application of PVA to high performance fibers with a high strength and a high modulus is an important goal from an industrial view point. The tensile strength, Young modulus, and optical birefringence (Δn) of the sPVA fiber drawn 30 times the original length and the aPVA fiber drawn 15 times the original length are summarized in Table 3. Although the draw ratio of the sPVA fiber is 1.5 times larger than that of the aPVA fiber, the strength and the Δn of the sPVA fiber were similar to those of the aPVA fiber. Though the modulus was higher for the sPVA fiber than for the aPVA fiber, the modulus of 38.1 GPa and strength of 1.43 GPa for the sPVA fiber of $\lambda = 30$ are not high enough to be considered as a high performance fiber. On the basis of the intrinsic birefringence (Δn_0) of 0.0518 for the fully orientated crystalline PVA [34], the orientation coefficient, f ($f = \Delta n/\Delta n_0$) of sPVA was 0.685, which is not very high. This is because the spherulites may rapidly form in the drawing process and prevent sPVA molecules from orienting due to strong intermolecular hydrogen bond. Thus, the conventional drawing methods using a hot oven may be difficult to make highly oriented PVA molecules with a high syndiotacticity. More detailed studies are needed to optimize the drawing method and conditions to obtain sPVA fibers having a higher strength and a higher modulus, which is now under investigation.

4. Conclusions

The properties of sPVA with $r = 69\%$ and aPVA with $r = 54\%$ were examined for the as-obtained, as-spun fiber, and drawn fiber samples. Most of the properties discussed in this study were greatly affected by the main-chain tacticity. sPVA was found to have higher melting point, crystallization temperature, and T_g compared with aPVA. The differences in the properties may be ascribed mainly to

differences in intermolecular hydrogen bonding of the PVAs that is caused by the change in tacticity although the effect of the intramolecular hydrogen bond may also be partially responsible. Although the analyses in this study focused on the static properties, dynamic mechanical analyses are under way to obtain a deeper insight into the structure–property relation of the PVAs.

Acknowledgements

This work was supported by the New Energy and Industrial Technology Development Organization (NEDO) under the Ministry of International Trade and Industry (MITI), Japan, through the grant for 'Precision Catalytic Polymerization' in the Project 'Technology for Novel High-Functional Materials' (1996–2000).

References

[1] Finch CA. Polyvinyl alcohol — developments. Chichester: Wiley, 1992.
[2] Fujii K. J Polym Sci Macromol Rev 1971;5:431.
[3] PVA no Sekai, Kyoto; Kobunshi Kankokai, 1992.
[4] Sakurada I. Polyvinyl alcohol fibers. New York: Marcel Dekker, 1985.
[5] Yamaura K, Matsuzawa S. Polyvinyl alcohol. Kyoto: Kobunshi Kankokai, 1991.
[6] Matsuzawa S, Sun L, Yamaura K. Koubunshi Ronbunshu 1991;48:691.
[7] Fukae R, Yamamoto T, Fujita Y, Kawatsuki N, Sangen O, Kamachi M. Polym J 1997;29:293.
[8] Fukae R, Yamamoto T, Sangen O, Saso T, Kako T, Kamachi M. Polym J 1990;22:636.
[9] Choi JH, Lyoo WS, Ghim HD, Ko SW. Colloid Polym Sci 2000;278:1198.
[10] Lyoo WS, Han SS, Yoon WS, Ji BC, Lee J, Cho YW, Choi JH, Ha WS. J Appl Polym Sci 2000;77:123.
[11] Haas HC, Emerson ES, Schuler NW. J Polym Sci 1956;22:291.
[12] Yamaura K, Tanigami T, Hayashi N, Kosuda K, Okuda S, Takemura Y, Itoh M, Matsuzawa S. J Appl Polym Sci 1990;40:905.
[13] Murahashi K, Nozakura S, Sumi M, Fuji S, Matsumura K. Koubunshi Kagaku 1966;23:550.
[14] Murahashi K, Nozakura S, Sumi M, Yuki H, Hatada K. Koubunshi Kagaku 1966;23:605.
[15] Sumi M, Matumura K, Ohno R, Nozakura S, Murahashi N. Koubunshi Kagaku 1967;24:606.
[16] Murahashi K, Nozakura S, Sumi M, Yuki H, Hatada K. Polym Lett 1966;4:65.
[17] Yamada K, Nakano T, Okamoto Y. Proc Japan Acad 1998;74 (B): 46.
[18] Yamada K, Nakano T, Okamoto Y. Macromolecules 1998;31:7598.
[19] Nagara Y, Yamada K, Nakano T, Okamoto Y. Polym J 2001;33:534.
[20] Mandelkern L. Crystallization of polymers. New York: McGraw-Hill, 1964.
[21] Avrami M. J Chem Phys 1939;7:1103.
[22] Avrami M. J Chem Phys 1940;8:212.
[23] Avrami M. J Chem Phys 1941;9:177.
[24] Monobe K, Fujiwara H. Kobunshi Kagaku 1964;21:179.
[25] Yamaura K. Kobunshi Kako 1992;41:73.
[26] Nagashima N, Matsuzawa S, Okazaki M. J Appl Polym Sci 1996;62:1551.
[27] Gagnaire D, Mancier D, Vincendon M. J Polym Sci, Polym Chem Ed 1980;18:13.
[28] Freddi G, Pessina G, Tsukada M. Int J Biol Macromol 1999;24:251.
[29] Ogasawara K, Yuasa K, Matsuzawa S. Makromol Chem 1976;177:3403.
[30] Fujii K, Mochizuki T, Ukida J, Matsumoto M. J Polym Sci, Part B 1963;1:697.
[31] Chatani Y, Takeda K, Matsuzawa S, Yamaura K. Polym Prepr Jpn 1985;34:800.
[32] Bunn CW. Nature 1948;161:929.
[33] Tubbs RK. J Polym Sci, Part A 1965;3:4181.
[34] Hibi S, Maeda M, Takeuche M, Nomura S, Shibata Y, Kawai H. Sen'i Gakkaishi 1971;27:41.